Electroluminescence of 2,4-bis(4-(2′-thiophene-yl)phenyl)thiophene in organic light-emitting field-effect transistors

Takahito Oyamada, Hiroyuki Sasabe, and Chihaya Adachi[a)]
Department of Photonics Materials Science, Chitose Institute of Science and Technology (CIST), 758-65 Bibi, Chitose, Hokkaido 066-8655, Japan

Suguru Okuyama and Noriyuki Shimoji
New Material Device R&D Center, Rohm Co., 21 Saiin Mizosaki, Ukyo, Kyoto 615-8585, Japan

Kazumi Matsushige
International Innovation Center (IIC), Kyoto University, Yoshida-Honmachi, Sakyo, Kyoto 606-8501, Japan

We succeeded in observing electroluminescence (EL) of 2,4-bis(4-(2′-thiophene-yl)phenyl)thiophene (TPTPT) as an active layer in an organic field-effect transistor (OFET). In particular, an OFET with a short channel of $d_{SD}=0.8$ μm demonstrated higher EL efficiency than one with a much longer channel ($d_{SD}=9.8$ μm). We observed a maximum EL quantum efficiency (η_{max}) of 6.4×10^{-3} % in the short-channel-length device at an applied source-drain voltage of $V_d=-100$ V and a gate voltage of $V_g=-40$ V. From the OFET characteristics, although the TPTPT layer demonstrated typical *p*-type operation, the occurrence of EL clearly indicated simultaneous hole and electron injection from the source and drain electronics, respectively, under high V_d and V_g. © *2005 American Institute of Physics.* [DOI: 10.1063/1.1870105]

Research on organic field-effect transistors (OFETs) using organic semiconductor materials[1–18] accelerated after a series of articles by Schön.[9–11] Although most of these articles were eventually withdrawn, the ideas he contained acted as a catalyst for advances in OFET research. In particular, reports on organic light-emitting FETs (OLEFETs) using an oligo-thiophene derivative, α-sexithiophene (α-6T),[1–4,10] stimulated great interest because they have a variety of potential applications in light-emitting devices, organic integrated circuits for optical interconnections, and organic laser diodes.

Recently, there have been several important findings on electroluminescence (EL) in OFETs. Heep *et al.* reported electroluminescence (EL) from a bottom-contact-type OFET with a benz[b]anthracene (tetracene) polycrystalline film as an active layer under a so-called *p*-type driving condition,[12] demonstrating double injection of holes and electrons from source and drain (SD) electrodes. Ahles *et al.* observed EL from poly(9,9-diethylhexyl-fluorene) (PF2/6) in a similar OFET structure.[13] Both letters suggested that considerable electron injection was produced by a high electrical field between the organic layer and an under-etched Au drain electrode, which induced a strong electrical field for electron injection. In addition, Misewich *et al.* observed emission of infrared light from an ambipolar FET using a carbon nanotube as an emitter.[14] More recently, Sakanoue *et al.* also succeeded in observing EL from a bottom-contact-type OFET using poly[2-methoxy-5-(2′-ethylhexyloxy)-1,4-phenylene vinylene] as an active layer, demonstrating that asymmetric source-drain electrodes of Al/Au greatly enhance EL efficiency.[15]

In this study, we demonstrated EL of 2,4-bis(4-(2′-thiophene-yl)phenyl)thiophene [TPTPT, Fig. 1(a)] as an active layer in an OFET. We focused on TPTPT since the oligothiophene derivatives, both as single crystals and thin films, have been widely studied as a potential FET material.[1–17] However, to date there have been no reports of EL using these thiophene derivatives. Here, we investigated the OLEFET characteristics of TPTPT using different channel lengths ($d_{SD}=0.8$ and 9.8 μm) between the source and drain electrodes and found that the OLET characteristics were strongly dependent on channel length.

Figure 1(b) shows a schematic view of the structure of the fabricated OLEFET device. A highly doped n^+-Si (100) wafer with a 320-nm-thick SiO$_2$ layer ($C_i=1.18\times10^{-8}$ F) was used as a gate electrode. Bottom-contact-type source and drain electrodes composed of Cr(0.5 nm)/Au(50 nm) were formed on the SiO$_2$/n^+-Si layer using conventional photolithography and lift-off techniques.[18] The channel lengths be-
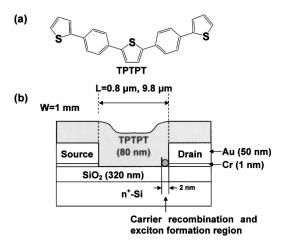

FIG. 1. (a) Molecular structure of TPTPT, (b) structure of organic light-emitting field-effect transistor (OLEFET). The area of carrier recombination and exciton formation used in the calculation of light out-coupling efficiency is indicated by a circle.

[a)]author to whom correspondence should be addressed; electronic mail: c-adachi@photon.chitose.ac.jp
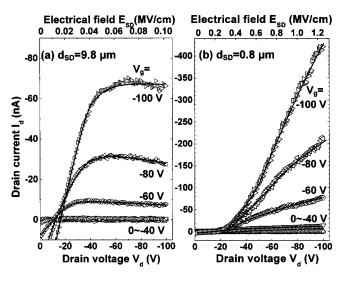
FIG. 2. Drain current (I_d) vs drain voltage (V_d) characteristics depending on channel length between source and drain electrodes, $d_{SD}=9.8$ μm (a) and 0.8 μm (b), in OLEFETs with TPTPT layer as active layer. Various gate voltages (V_g), 0 V ($\bigcirc$), -20 V ($\triangle$), -40 V ($\triangledown$), -60 V ($\diamond$), -80 V ($\triangleleft$) and -100 V ($\triangleright$), were applied in these devices.

FIG. 3. Luminance (L) vs drain voltage (V_d) characteristics depending on channel length between source and drain electrodes, $d_{SD}=9.8$ μm (a) and 0.8 μm (b), in OLEFETs with TPTPT layer as active layer. Various gate voltages (V_g), 0 V ($\bigcirc$), -20 V ($\triangle$), -40 V ($\triangledown$), -60 V ($\diamond$), -80 V ($\triangleleft$) and -100 V ($\triangleright$), were applied in these devices.

tween the source and drain electrodes were 0.8 and 9.8 μm, with a width of 1 mm. After the photolithography process, the substrate was degreased with acetone and isopropanol and cleaned before being loaded into a evaporation system. An 80-nm-thick TPTPT film as an active layer was deposited on the Au electrodes in a vacuum of $<1\times10^{-3}$ Pa.

All measurements were carried out in a vacuum of $\sim1\times10^{-3}$ Pa at room temperature. The dependence of the drain current (I_d) drain voltage (V_d) luminance (L) characteristics on the gate voltage (V_g) were measured using a HP4145 semiconductor parameter analyzer with the quantum efficiency directly obtained by centering a highly sensitively calibrated photon counter (HAMAMATSU, C767) on to the OLEFETs. The V_d was scanned from 10 to -100 V in -1 V steps and the V_g was scanned from 0 to -100 V in -20 V steps.

Figure 2 shows the dependence of the I_d-V_d characteristics on both channel lengths, $d_{SD}=9.8$ μm (a) and 0.8 μm (b), respectively. The OLEFET with $d_{SD}=9.8$ μm (a) showed typical unipolar FET characteristics. The I_d-V_d characteristics showed linear behavior in the low V_d region ($\lesssim-30$ V) and typical saturation behavior in the high V_d region ($\gtrsim-40$ V), indicating the formation of a pinch-off region near the drain electrode under saturation conditions ($V_d\gtrsim-40$ V). However, the OLEFET with a short channel (b) demonstrated unusual I_d-V_d characteristics. The I_d progressively increased and no saturation behavior was observed even with $V_d=-100$ V. Here, we suggest that a very high electrical field approaching ~1 MV/cm, corresponding to the electrical field in which conventional organic light-emitting diodes (OLEDs) operate, was applied between the source and drain electrodes in the device (b) when $V_d\sim-100$ V, although the maximum electrical field between the source and drain electrodes was only ~0.1 MV/cm in the other device (a). Therefore, it is probable that the high electrical field significantly modified the energy barrier in the vicinity of the drain electrode, leading to efficient electron injection and carrier recombination in the pinch-off region.

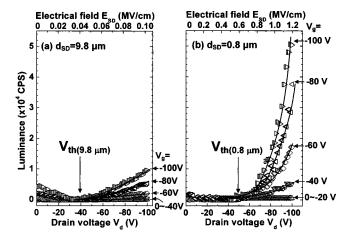Figure 3 shows the dependence of the L-V_d characteristics on the channel length, $d_{SD}=9.8$ μm (a) and 0.8 μm (b),

respectively. First, we discuss the FET characteristics of the latter device (b). The OLEFET with $d_{SD}=0.8$ μm (b) showed pronounced light emission with a maximum light intensity of over 50 000 CPS, which was ~5 times higher than that of the other device (a), indicating that the application of a high electrical field approaching $\sim$ MV/cm greatly enhanced the electron injection efficiency. From the onset of the EL, electron injection started above the threshold voltage $V_{th}\sim-50$ V, although there was no noticeable change in the I_d-V_d characteristics around $V_d\sim-50$ V, as shown in Fig. 2(b). We also observed an increase in light emission with increasing V_g. Appreciable EL was observed with a V_g higher than -40 V. It increased steeply with the higher V_g, indicating that the application of V_g intensified the local electrical field in the vicinity of the drain electrode, leading to the enhancement of electron injection. In the case of $d_{SD}=9.8$ μm, on the other hand, the onset voltage (V_{th}) of EL was observed around $V_d\sim-40$ V, which almost corresponded to the turning point from the linear to the saturation region as shown in Fig. 2(a), indicating that electron injection began after the formation of the pinch-off region.

Figure 4 shows the dependence of the external quantum efficiency (η_{ext})-V_d characteristics on the channel length, $d_{SD}=9.8$ μm (a) and 0.8 μm (b), respectively. η_{ext} gradually increased with increasing V_d in all the devices. The OLEFET with the short channel length ($d_{SD}=0.8$ μm) (b) showed a maximum η_{ext} of 6.4×10^{-3}%, which was ~9 times higher than that of the other device (a), indicating that the formation of the short SD length significantly enhanced η_{ext} due to efficient electron injection from the drain electrode. η_{ext} also progressively increased with an increase in V_d. Since TPTPT shows p-type FET characteristics, the major carrier in the TPTPT layer is holes and the electron injection efficiency probably increased with increasing V_d. In addition, we observed that the OLEFET with $d_{SD}=0.8$ μm (b) showed a pronounced decrease in η_{ext} with increasing V_g. This behavior could be related to exciton quenching by the high electrical field,[19] or exciton annihilation under the high current density.[20] This issue is being given further consideration.

Here, we discuss the possible mechanism of electron injection in the OLEFETs. Our results clearly demonstrated electron injection from an Au electrode, which is usually an
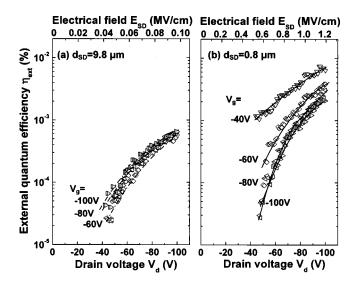
FIG. 4. External quantum efficiency (η_{ext}) vs drain voltage (V_d) characteristics depending on channel length between source and drain electrodes, $d_{SD}=9.8$ μm (a) and 0.8 μm (b), in OLEFETs with TPTPT layer as active layer. Various gate voltages (V_g), -40 V ($\triangledown$), -60 V ($\diamond$), -80 V ($\triangleleft$) and -100 V ($\triangleright$), were applied in these devices.

inefficient electron injection cathode in OLEDs, since the large electron-injection barrier (3.2 eV) between the Au (work function of 4.5 eV)[18] electrode and the lowest unoccupied molecular orbital level of the TPTPT deposited film ($E_a=1.3$ eV) prevents efficient electron injection. Therefore, we suppose that an unusually high electrical field must be generated between the organic layer and the drain electrode, which will promote electron injection. Probably, a very high electrical field formed in the pinch-off region in the vicinity of the drain electrode reduces the electron-injection barrier. Under these circumstances, electron injection by means of Fowler–Nordheim tunneling injection,[21] the Zener effect,[22] or hot-carrier impact ionization[23,24] can be expected.

Finally, we estimate the carrier-injection balance factor (γ), i.e., the hole/electron ratio, to examine the rate-determining process for EL efficiency in this device. We used a simulation program of LightTools[25] to estimate the light out-coupling efficiency (η_p) in the OFET structure as shown in Fig. 1(b) ([refractive index: n, reflectivity index: r and transmittance: t]; active layer (TPTPT): $n \approx 1.9$ and $t=100\%$ at $\lambda=507$ nm, SD electrodes (Au): $r \approx 60\%$, insulator (SiO$_2$): $n \approx 1.5$ and $t=100\%$ at $\lambda=350$–800 nm, gate electrode (n^+Si): $n \approx 3.6$ and $r \approx 30\%$ at $\lambda=400$–800 nm). In this estimation, multiple interference effect has not been considered. It was assumed that carrier recombination and exciton formation occurred in the position marked, which was 2 nm away from the drain electrode and on the SiO$_2$ layer as shown in Fig. 1(a). With these parameters, we obtained an approximate η_p of $\sim 6\%$. Since γ^{26} is obtained as follows:

$$\gamma = \frac{\eta_{ext}}{\eta_r \Phi_{PL} \cdot \eta_p}$$

and the maximum η_{ext} is $6.4 \times 10^{-3}\%$ in $d_{SD}=0.8$ μm and $7.1 \times 10^{-4}\%$ in $d_{SD}=9.8$ μm, with a fluorescence efficiency (Φ_{PL}) of $8 \pm 1\%$ in a deposited film of TPTPT, and a η_p of

$\sim 6\%$, and assuming an exciton-generation efficiency (η_r) of $\sim 25\%$ due to the singlet exciton characteristics of TPTPT, we obtained a maximum γ of $\sim 0.6\%$ in $d_{SD}=9.8$ μm and $\sim 5\%$ in $d_{SD}=0.8$ μm, suggesting that the electron injection efficiency was still very low.

In summary, we observed EL from an OFET with a TPTPT layer as the active layer. We demonstrated a significant improvement in electron injection and EL efficiency by using a short channel length of $d_{SD}=0.8$ μm in a FET structure. However, this electron-injection efficiency was still low compared with the hole-injection efficiency. In a subsequent study, we demonstrate that η_{ext} can be improved significantly by selecting appropriate organic materials and altering the source and drain electrodes configuration.

[1] G. Horowitz, D. Fichou, X. Peng, Z. Xu, and F. Garnier, Solid State Commun. **72**, 381 (1989).
[2] F. Garnier, G. Horowitz, X. Z. Peng, and D. Fichou, Synth. Met. **45**, 163 (1991).
[3] A. Dodabalapur, L. Torsi, and H. E. Katz, Science **268**, 270 (1995).
[4] Z. Bao, A. Dodabalapur, and A. J. Lovinger, Appl. Phys. Lett. **69**, 4108 (1996).
[5] A. R. Brown, C. P. Jarrett, D. M. de Leeeuw, and M. Matters, Synth. Met. **88**, 37 (1997).
[6] D. X. Wang, Y. Tanaka, M. Iizuka, S. Kuniyoshi, K. Kudo, and K. Tanaka, Jpn. J. Appl. Phys., Part 1 **38**, 256 (1999).
[7] H. Ishii, K. Sugiyama, E. Ito, and K. Seki, Adv. Mater. (Weinheim, Ger.) **11**, 605 (1999).
[8] X. M. Hong, H. E. Katz, A. J. Lovinger, B. Wang, and K. Raghavachari, Chem. Mater. **13**, 4686 (2001).
[9] J. H. Schön, Ch. Kloc, R. C. Haddon, and B. Batlogg, Science **288**, 656 (2000).
[10] J. H. Schön, A. Dodabalapur, Ch. Kloc, and B. Batlogg, Science **290**, 963 (2000).
[11] J. H. Schön, Ch. Kloc, and B. Batlogg, Nature (London) **406**, 704 (2000).
[12] A. Heep, H. Heil, W. Weise, M. Ahles, R. Schmechel, and H. von Seggern, Phys. Rev. Lett. **91**, 157406 (2003).
[13] M. Ahles, A. Hepp, R. Schmechel, and H. von Seggern, Appl. Phys. Lett. **84**, 428 (2004).
[14] J. A. Misewich, R. Martel, Ph. Avouris, J. C. Tsang, S. Heinze, and J. Tersoff, Science **300**, 783 (2003).
[15] T. Sakanoue, E. Fujiwara, R. Yamada, and H. Tada, Appl. Phys. Lett. **84**, 3037 (2004).
[16] A. R. Brown, C. P. Jarrett, D. M. de Leeeuw, and M. Matters, Synth. Met. **88**, 37 (1997).
[17] H. Yanagi, Y. Araki, T. Ohara, S. Hotta, M. Ichikawa, and Y. Taniguchi, Adv. Funct. Mater. **13**, 767 (2003).
[18] T. Oyamada, H. Sasabe, and C. Adachi, IEEJ Trans. Electronics, Information and Systems, **124C**, 1216 (2004).
[19] T. Oyamada, T. Sato, H. Sasabe, and C. Adachi, 56th Spring Meeting of the Japan Society of Applied Physics and Related Societies, 2004, Extended Abstract, Paper No. 30a-ZN-2.
[20] M. A. Baldo, C. Adachi, and S. R. Forrest, Phys. Rev. B **62**, 10967 (2000).
[21] R. H. Fowler and L. Nordheim, Proc. R. Soc. London, Ser. A **119**, 173 (1928).
[22] C. Zener, Proc. R. Soc. London, Ser. A **145**, 523 (1934).
[23] G. Juska and K. Arlauskas, Phys. Status Solidi A **59**, 389 (1980).
[24] K. K. Thorber, J. Appl. Phys. **52**, 279 (1981).
[25] M. J. Hayford and S. R. David, J. Phys. I **3130**, 209 (1997).
[26] C. Adachi, M. A. Baldo, M. E. Thompson, and S. R. Forrest, J. Appl. Phys. **90**, 5048 (2001).